ACS APPLIED POLYMER MATERIALS

pubs.acs.org/acsapm Article

Blends of Poly(butylene glutarate) and Poly(lactic acid) with Enhanced Ductility and Composting Performance

Apisata Holt, Yutian Ke, Jessica A. Bramhall, Grant Crane, Joe B. Grubbs, III, Evan M. White, Jessica Horn, and Jason Locklin*

Cite This: ACS Appl. Polym. Mater. 2021, 3, 1652−1663 Read Online

ACCESS | Metrics & More | Article Recommendations | Supporting Information

ABSTRACT: Blends of poly(lactide) (PLA) with poly(butylene glutarate) (PBG) have been investigated with a focus on the improvement of PLA brittleness and an enhancement of the degradation rate under industrial composting conditions. PBG was synthesized by melt polycondensation between 1,4-butanediol (C4) and glutaric acid (C5). The effect of the odd carbon atom number in the dicarboxylic acid monomer caused a decrease in melting temperature (T_m) and crystalline content, and subsequently an increase in composting degradation rate. The films of PLA blended with various compositions of PBG were prepared by solution casting and hot pressing. Physical, mechanical, and viscoelastic behavior along with morphology of the blends were investigated using a variety of techniques. All PLA/PBG blends showed a decrease in both glass transition temperature (T_g) and tensile strength, but showed an increase in the % elongation at break. The composting degradability of PBG and selected PLA/PBG blends were investigated using respirometry. Considering all of the analyses performed, adding PBG to PLA improved the brittleness of PLA and accelerated the rate of degradation in industrial composting. PLA/PBG blends exhibited higher ductility than the blends of PLA with poly(butylene succinate), a polymer commonly compounded with PLA in many thermoplastic applications. The compatibility of PBG in a PLA matrix was dependent on the concentration of PBG in the PLA matrix, with phase separation evident above 3 wt %.

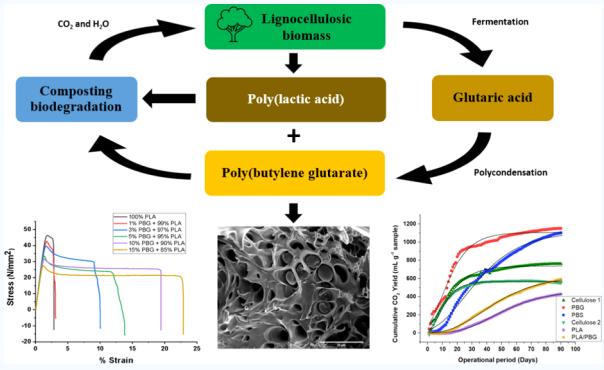

KEYWORDS: *bio-based aliphatic polyester, condensation polymerization, polymer blend, phase separation, composting degradation, modified Gompertz model*

1. INTRODUCTION

In recent years, the development of bio-based polyesters has attracted considerable attention due to monomer sourcing from renewable resources (and thus CO_2 sequestration), along with selective abiotic and biotic degradation under certain environmental conditions.[1,2] Among these polyesters, poly(lactide) (PLA) is one of the most well-studied thermoplastics and a commercial alternative for some conventional petroleum-based polymers.[3,4] PLA is an aliphatic polyester, its monomer lactide is produced through the fermentation of renewable resources, and its composting degradation products are water and carbon dioxide when carried out in aerobic conditions at temperatures at or above the glass transition temperature. PLA is used in many market sectors for both disposable and durable goods including packaging, textile, automotive, additive manufacturing, and medical applications. PLA exhibits good mechanical properties as well as easy processability.[5,6] Its tensile strength and tensile modulus are similar to poly(ethylene terephthalate) (PET).[7−9] PLA can be conventionally processed using extrusion, injection molding, blow molding, and also fiber spinning.

The well-known drawbacks of PLA such as brittleness, low heat deflection temperature, poor impact resistance, and slow degradation rate at end-of-life are major disadvantages for commercial applications in the single-use item and packaging industries.[10,11] Current research on PLA modification has been focused on improving the mechanical and thermal properties by either copolymerization or physical blending, with compounding being the more practical and cost-effective method to obtain the desired properties.[12] PLA blends with nanocomposites and nanofibrils have also been explored to overcome the brittleness of PLA. There have been several studies aimed at controlling the phase morphology of these reenforcing nanocomposites such as adding PBS and PBAT nanofibrils in the PLA matrix.[13,14] Moreover, certain small-

Received: January 18, 2021
Accepted: February 12, 2021
Published: February 25, 2021

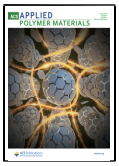

https://dx.doi.org/10.1021/acsapm.1c00078
ACS Appl. Polym. Mater. 2021, 3, 1652−1663

molecule plasticizers such as citrate esters,[15] triacetine,[16] and epoxidized soybean oil,[17] or other polymers such as polyethylene glycol,[18,19] poly(caprolactone),[20] poly(butylene succinate),[21] and poly(butyleneadipate-co-terephthalate)[22] have been observed to be effective additives at improving flexibility and toughness. The role of these additives is to enhance the mobility of polymer chains as well as increasing elongation at break of the polymer.[23]

Organic plasticizers with low molecular weight and high to moderate vapor pressure have the tendency to volatilize during extrusion or eventually migrate from the polymer matrix of the formed article under certain conditions. The loss of plasticizers can lead to functional failures and contaminate the surrounding medium, which limits their use in areas like food packaging and biomedical applications. Polymeric plasticizers have been used to hinder plasticizer migration due to their high molecular weight, better water resistance, excellent oil, and solvent extraction and longer service life.[24] More specifically, many polyesters also have the characteristics of low toxicity and safety.[25] It is reported that blending PLA with ductile polyesters that exhibit lower glass transition temperature (T_g) such as poly(butylene succinate) (PBS) can improve PLA brittleness.[21] PBS is an aliphatic polyester synthesized by melt polycondensation of 1,4-butanediol (C4) and succinic acid (C6). It is semicrystalline with a glass transition temperature (T_g) of about −30 °C and a melting temperature (T_m) around 114 °C. As a soft component in binary PLA/PBS blends, it is reported that PBS acts as a stress concentrator preventing brittle failure and enabling ductile yield.[26] The elongation at break of PLA/PBS blends increases gradually with increasing PBS content. However, without the use of reactive extrusion,[27] the brittleness of PLA does not significantly improve until the PBS content is very high, at 80−90 wt %.[28,29]

In terms of degradation in aerobic conditions, polyesters such as PLA and PBS degrade through a two-step process.[30,31] In the first step, hydrolytic degradation occurs under an appropriate temperature and moisture environment resulting in a substantial decrease in molecular weight. Then, enzymatic degradation by certain microorganisms can metabolize these lower-molecular-weight (monomeric and possibly oligomeric) components to biomass, carbon dioxide, and water. The hydrolysis process of the PLA and PBS depends on various factors including the morphology, degree of crystallinity, presence of additives, and conditions in the degradation environment such as pH, humidity, and temperature.[32] Importantly, water absorptivity plays a significant role in the hydrolysis process. The degradation of PLA in soil is slow partly because of its hydrophobicity, where water is unable to easily penetrate the PLA matrix.[33] The degradation of PLA in industrial compost is much faster than in soil conditions since the temperature of the inoculum can rise above or around the T_g. The elevated temperature environments (~50 to 60 °C) in industrial compost help to increase chain mobility in the amorphous phase, with a subsequent increase in the diffusion rate of water.[34] The addition of PBS to PLA has also resulted in accelerated hydrolytic degradation. It has been reported that the relatively higher hydrophilic character of PBS compared to PLA and immiscible PBS particles enhance the hydrophilicity and introduce gaps/voids in blends, providing channels for water penetration.[27,35]

Poly(butylene glutarate) (PBG) is also an aliphatic polyester but synthesized from 1,4-butanediol (C4) and glutaric acid (C5). The chain length of diacids and the even−odd effect on the chemical structure of the aliphatic polyesters ultimately determine their thermal properties and crystallinity.[36] From a material point-of-view, the effect of an odd-numbered diacid can influence the number of hydrogen bonds per gram of polymer, leading to a decrease in T_m and percent crystallinity. Polyesters made from even−even carbon monomers (such as PBS) display relatively high T_m and crystallinity, and the degree of crystallinity of the polyester plays an important role in the degradation process. Low crystallinity with a higher fraction of the amorphous phase is usually more easily degraded by hydrolysis due to faster rate of water diffusion.[37] Nowadays, odd or even diacids and diol monomers can be produced on a large scale from renewable plant resources such as corn starch and sugarcane.[38,39] The fermentation technology alternative to petroleum-derived products is made possible in the biosynthetic routes of succinic acid[38] and, more recently, glutaric acid.[40,41] The potential for bio-based production to replace petroleum-based production of these monomers has attracted lots of attention because it is a sensible approach for achieving economic and environmental sustainability.[42]

In view of thermal properties and degradation rate, the use of PBG can offer several advantages such as improving brittleness and increasing degradation rate to PLA blends. In this work, the odd−even aliphatic polyester PBG was first synthesized through polycondensation/transesterification and fully characterized in terms of thermal and degradation properties. Then, the blends of PLA and PBG were prepared with various compositions via solution casting, and the influence of PBG on the thermal, mechanical, and morphological properties of the PLA blends was investigated. The impact of PBG on composting biodegradation was also examined. The result from this study will offer not only an alternative to petroleum-based additives but improvements in both mechanical properties and the rate of degradation at much lower blend ratios than other aliphatic polyesters.

2. EXPERIMENTAL SECTION

2.1. Materials. PLA (Ingeo 3251D, Nature Works, LLC.) was obtained in resin form from Danimer Scientific. The T_g was approximately 60 °C, and the T_m was approximately 170 °C. According to the manufacturer's data sheet, the exact proportion of D, L stereoisomer level of monomer was not specified. PBS (FZ91PM) in pellet form was supplied by PTT MCC Biochem Co., Ltd. (Thailand). It had a T_g about −30 °C and a T_m about 114 °C. Glutaric acid and zirconium (IV) butoxide ($Zr(OBu)_4$) were purchased from Sigma-Aldrich. 1,4 Butanediol was purchased from Alfa Aesar and HPLC grade chloroform ($CHCl_3$) was purchased from JT Baker. Sigmacell cellulose (type 101) used as received in powder form was purchased from Sigma-Aldrich. This cellulose powder was used as a positive control to monitor microbial activities based on ASTM standard D5338-15 for composting the biodegradation test.[43]

2.2. PBG Synthesis and Characterization. PBG was prepared by copolymerization of glutaric acid and 1,4 butanediol through a two-step procedure using a rotary evaporator equipped with a condensation-collecting flask, a silicon oil bath, a nitrogen inlet, and a vacuum system controller. The molar ratio of diacid to diol was 1:1.01, and the catalyst was 0.08 wt % of the total monomers.

Briefly, 210 g (1589 mmol) of glutaric acid and 145 g (1609 mmol) of 1,4 butanediol were added together into a 500 mL round-bottom flask. The monomer mixture was heated to 150 °C for 1 h (agitated at 25 rpm) under a constant stream of nitrogen at atmospheric pressure to completely melt the monomers and remove all oxygen. After this time, the agitation and temperature of the mixture were raised to 50 rpm and 165 °C, respectively. The vacuum pressure was gradually

https://dx.doi.org/10.1021/acsapm.1c00078
ACS Appl. Polym. Mater. 2021, 3, 1652−1663

reduced from atmospheric pressure to 100 Torr over a period of 3 h to prevent excessive foaming and avoid monomer evaporation during polymerization. The water byproduct was collected and removed from the reaction vessel.

Then, the reaction pressure was slowly reduced to 1 Torr and the reaction mixture was continuously agitated for 16 h. Subsequently, the number of carboxylic acid end groups (acid number) was determined by standard titration in dioxolane with potassium hydroxide and phenolphthalein indicator (see the Supporting Information). When the acid number (AN) of the product was lower than 30, $Zr(OBu)_4$ (0.3 mL, 0.78 mmol) was added as a catalyst and continued to react for additional 12 h to obtain a product of high molecular weight. The final product was cooled to room temperature and freeze-dried for 24 h.

The structure of PBG was determined by proton nuclear magnetic resonance (^{1}H NMR) in $CDCl_3$ (Varian Inova 600 MHz spectrometer). The molecular weight and polydispersity index (PDI) of PBG samples were measured at 40 °C by gel permeation chromatography (GPC). The GPC system included an automatic sampler (Shimadzu, SIL-20A), two pumps (Shimadzu, LC-20AD), a column oven (Shimadzu, CTO-20A), an ultraviolet detector (Shimadzu, SPD-20 A), and a refractive index detector (Shimadzu, RID-10A). $CHCl_3$ was used as the mobile phase at a flow rate of 1.0 mL/min, and the molecular weight is reported relative to polystyrene standards. Thermogravimetric analysis (TGA) was performed on a Discovery TGA (TA Instruments) to obtain the decomposition temperature of PBG by heating from 30 to 500 °C at a rate of 3 °C/min under nitrogen atmosphere. The thermal properties and degradability of PBG were investigated using differential scanning calorimetry (DSC) on a DSC 250 (TA Instruments) and a 12-channel respirometer (ECHO instruments).

2.3. Preparation of Blends. The films of PLA/PBG blends and PLA/PBS blends were prepared by solution casting at various compositions. The composition ratios of the PBG and PBS in the blends were 0, 1, 3, 5, 10, and 15 wt %. PLA and PBG (or PBS) (approximately 2 g total polymer) were dissolved into 15 mL of $CHCl_3$. The mixtures were stirred at 350 rpm for 12 h before casting in a clean glass Petri dish (10 cm in diameter). The solvent was allowed to evaporate for 24 h at room temperature. The cast films were then removed from the Petri dish and air-dried at room temperature for 12 h.

To make uniform films with a thickness 100 ± 5 μm, a hydraulic press with heated platens (Carver, 4386) was used at 175 °C. The cast films were first placed between the platens without any pressure for 3 min; then, the films were pressed for 1 min at 500 psi. The specimens were removed from the press and cooled at room temperature (approximately 1 min). The final film thickness was measured with digital calipers. All films were stored in a desiccator for further analysis.

3. CHARACTERIZATION OF BLENDS

3.1. Differential Scanning Calorimetry (DSC). DSC measurements were performed on a DSC 250 (TA Instruments) under a nitrogen atmosphere. Specimen weighing approximately 5−6 mg were heated at a rate of 10 °C/min from 25 to 200 °C and held isothermally at 200 °C for 1 min to eliminate thermal history. They were then cooled to −80 °C at 10 °C/min and held isothermally for 1 min before a second heating step. The glass transition temperature (T_g), cold crystallization temperature (T_{cc}), and melting temperature (T_m) of the PLA blends were determined using the second heating curve.

3.2. Dynamic Mechanical Analysis (DMA). DMA was conducted on a DMA Q800 (TA Instruments). All films were cut into rectangular shapes using a punch (25 mm × 5.3 mm) from 100 ± 5 μm thick films. The specimens were gripped by tension clamps with a clamp compliance of about 4 in.lb. DMA multifrequency strain analysis with oscillations of 20 μm amplitude at 1 Hz was conducted. The temperature was ramped from 30 to 120 °C at 3 °C/min. The storage modulus, loss modulus, and tan δ were analyzed.

3.3. Tensile Test. The tensile properties of the neat PLA and the blends were measured using a tensile tester (Shimadzu, AGS-X series). Films were cut into dog-bone shapes using a die-cutter (Qualitest, ASTM-D1708-96-MET). All specimens were tested at room temperature with a cross-head speed of 5 mm/min.

3.4. Atomic Force Microscopy (AFM) and Atomic Force Microscopy-Infrared Spectroscopy (AFM-IR). PLA and polymer blend morphologies were examined by PeakForce Quantitative Nanomechanical Property Mapping (PF-QNM) on a Bruker Multimode Atomic Force Microscope. Image processing and data analysis were performed with the NanoScope Analysis software. The thin films of PLA and the blends were prepared by spin coating onto silicon wafers coated with native oxide (UniversityWafer, Inc.). The silicon wafers were cut into 2 cm × 2 cm squares and sonicated for 5 min with hexane, isopropyl alcohol, acetone, and water, followed by drying with a stream of nitrogen. The mixtures of polymer with various blend ratios (1−15 wt % PBG) were dissolved in $CHCl_3$ to produce 20 mg/mL solution. The thin films were then fabricated at room temperature with a spin speed of 1500 rpm using 200 μL of the mixture. Film thickness was measured using spectroscopic ellipsometry (J.A. Woollam, M-2000 V).

The AFM-IR measurements were carried on a NanoIR3 system (Bruker) in contact mode. The AFM-IR images were recorded with a contact mode tip (Anasys Instruments Inc.), which has a resonance frequency of 13 ± 4 kHz and a spring constant of 0.07−0.4 N/m. The AFM height images were acquired simultaneously with IR maps at ambient conditions. IR maps at 1730 and 1760 cm^{-1} wavenumbers were obtained to study the phase-separated morphology of the films. These single IR radiation images were recorded with a scan rate of 0.5 Hz and a resolution of 512 × 256 pixels.

3.5. Scanning Electron Microscope (SEM). The phase morphology of the fracture surface of the tensile bar was investigated using a FEI Teneo field emission-SEM at an accelerating voltage of 5 kV with a spot size of 7. Specimen were cut from the fracture surface of the tensile bar, fixed on pucks with conductive tape such that the cross section could be observed. The three-dimensional image of sample geometry fixed on the puck is illustrated in Figure S1. The fracture surfaces were sputter-coated with a gold/palladium coating using a LEICA EM ACE200 high vacuum sputter coater. The thickness of the Au/Pd layer was 6 nm.

3.6. Composting Biodegradation Test. All composting biodegradation tests were divided into two sets of experiments based on two different objectives. The degradation studies of PBS and PBG were first conducted to assess the effects of the even or odd carbon monomers on the rate of degradation. Then, the degradation studies of PLA and selected PLA blended with 15 wt % of PBG were performed to determine the effect of PBG on PLA degradation. Each experimental set was carried out in a 12-channel respirometer (ECHO instruments) under aerobic conditions at 58 °C for 90 days. The air was pumped into each reactor channel with a flow rate of 180 mL/min. The amounts of CO_2 emission from the outlet gas were analyzed every 2 h using a built-in gas sensor.

Two sets of compost inoculum were collected from industrial-scale compost facility located at the University of

https://dx.doi.org/10.1021/acsapm.1c00078
ACS Appl. Polym. Mater. 2021, 3, 1652−1663

Scheme 1. Synthetic Scheme for the Formation of PBG by Polycondensation of Glutaric Acid and 1,4 Butanediols

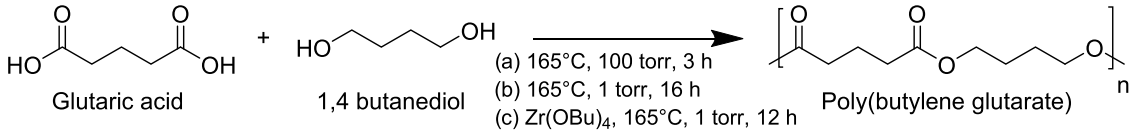

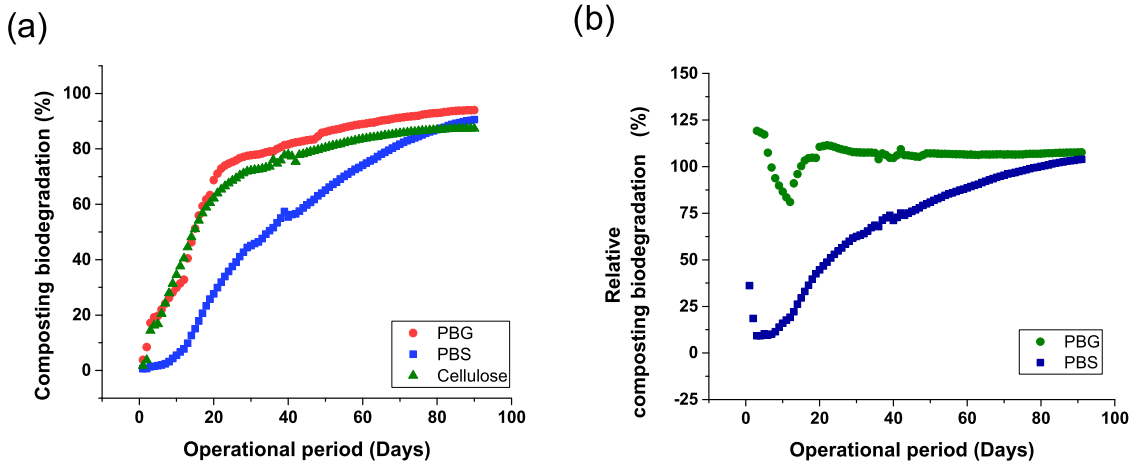

Figure 1. Composting biodegradation of PBG and PBS under ASTM D5338. (a) Composting biodegradation; (b) relative composting biodegradation.

Georgia, Athens, GA. These two compost sets were about 4−5 months old derived from composting the organic fraction of green waste, forest residue, food waste, and livestock manure. The temperature in the composting pile (50 cm depth) while collecting was 51 °C for the first set and 53 °C for the second set. Both sets of compost were sieved using a 4.75 mm screen (Sieve No. 4) to discard any large items such as stone, wood, and glass. The properties of fine and homogeneous compost such as pH, volatiles, and total solids were measured by pH probe and thermogravimetric analysis. Carbon and nitrogen contents of the two compost sets and samples were measured using the method described in Kristen (Table S1).[44]

Approximately 250 g of fine and homogeneous compost inoculum was introduced into 12 reactors. In each experimental set, samples were run in three replicates composed of 5 g of two test materials, 5 g of cellulose (positive reference), and blank (control), which is compost inoculum only. For the first degradation experiment, synthesized PBG was cut into small pieces and sieved using Sieve No. 4. PBS was dissolved in $CHCl_3$ and precipitated in methanol and sieved using Sieve No. 4. For the second degradation experiment, both PLA and 15 wt % PBG/PLA films were cut into a size of 25 mm × 25 mm. In both experiments, cellulose was used as received in powder form.

The compost inoculum in all reactors was stirred weekly to prevent clumping and provide an even distribution of moisture. Water was added into the reactors as necessary to maintain a constant moisture level and prevent drying of the compost inoculum. The actual carbon dioxide (CO_2) emission from each sample was measured and calculated by subtracting the average CO_2 production from the blank. The composting biodegradability was calculated from the ratio of actual CO_2 emission to the theoretical amount of the evolved CO_2 in each test period according to the testing method from ASTM standard D5338-15.[43] For a better understanding of the degradation kinetics, the data were fitted to a Modified Gompertz model which was developed to describe the cumulative CO_2 generation curve from each reactor.[45−48] The methods calculating biogas production and the modified Gompertz model fitting are presented in the Supporting Information.

4. RESULTS AND DISCUSSION

4.1. Synthesis and Characterization of PBG. PBG was synthesized following the two-step melt polymerization process of glutaric acid and 1,4 butanediol (Scheme 1). In the beginning, esterification reactions between acid and alcohol dominate and generate low-molecular-weight oligomers. In this stage, the viscosity of the melt is low enough that phase equilibrium can be achieved with a good agitation.[49] The reaction mixture was heated to 165 °C and mixed at 50 rpm under the reduced pressure of 100 Torr for 3 h until no more water was removed from the reaction mixture. The viscosity of the polymer melt increased with reaction time, and the removal of the small molecules becomes more difficult, limited by mass transfer.[50] The vacuum pressure was lowered further (1 Torr) and heated for an additional 16 h. The number average molecular weight (Mn), weight average molecular weight (Mw), and polydispersity index (PDI) of PBG at this stage was 7384 g/mol, 11,308 g/mol, and 1.53, respectively. In the second step, transesterification was carried out using a Lewis acid catalyst, ($Zr(OBu)_4$), for an additional 12 h to yield a higher-molecular-weight polymer (Mn = 24 229 g/mol, Mw = 40 560 g/mol, and PDI =1.67).

^{1}H NMR analysis was performed to verify the chemical structure of PBG (Figure S2), where the butylene subunit resonance signals of the *A* and *B* protons were observed at 4.10 and 1.70 ppm, respectively. The signal of a and b protons from the glutarate subunit is located at 2.37 and 1.94 ppm, respectively. The thermal decomposition of PBG was determined by the percentage of the mass loss versus temperature using TGA. From the thermogram curve (Figure

https://dx.doi.org/10.1021/acsapm.1c00078
ACS Appl. Polym. Mater. 2021, 3, 1652−1663

S3), the degradation temperature of PBG was approximately 372 °C measured by onset extrapolation. The thermal properties of PBG are shown in Figure S4. From the DSC curve, the T_g and T_m of PBG is −60 and 38 °C, respectively. It is noted that the T_m of PBG is significantly lower than that of PBS (∼114 °C), which limits its application as a stand-alone thermoplastic.

Then, PBG was compared to PBS to evaluate the effects of the odd or even carbon monomers on the rate of degradation. The compost inoculum that was used in this experiment had pH of 8.2, total solid of 54.2% of the wet solid, and volatile solid of 17.0% of the wet solid. The total carbon to nitrogen ratio (C/N) of the compost inoculum was 15.3. The carbon and nitrogen contents of PBG were C = 60.1% and N = 0.02% and PBS were C = 59.7% and N = 0.02%, respectively. Each sample was run in triplicate. Figure 1 shows the respirometry data. In an operation time of 30 days, the cellulose positive control reached 72.1% biodegradation on average. PBG and PBS achieved 77.7 and 45.1% biodegradation under the same period of evaluation. The % relative composting biodegradation of PBG and PBS was 107.7 and 62.5 when normalized against cellulose. All data for % composting biodegradation and % relative composting biodegradation after 60 and 90 days are reported in Table S2.

The result of the biodegradation experiments demonstrates that PBG degraded faster than PBS and cellulose under the conditions of ASTM D5338, which simulate industrial composting. The replacement of succinic acid (C4) by glutaric acid (C5) significantly decreases the T_m from 114 to 38 °C, which increases the degradation rate from 60 to 24 days. This observation could be described to the fact that odd or even number of carbon atom monomers and orientation of dipole alignment in these two polyesters (PBG and PBS) influence crystal structure.[36,51−53] In polyesters with an even number of carbon atoms between carbonyl groups contains close layers of dipoles of the opposite direction. This has the effect of canceling the local polarization. In polyesters with an odd number of carbon atoms between carbonyl groups, all of the dipoles are arranged in an identical direction, which repel each other, decreasing the overall stability.[53] Scheme 2 illustrates the arrangement of the polar layers for PBS and PBG.[53,54] The overall effect of odd carbon numbers is a decrease in crystallinity and T_m. In this regard, the crystallinity and T_m of polyesters have a strong effect on the abiotic (hydrolytic) and biotic degradation rate. The lower T_m of PBG is excellent for composting biodegradation, since the elevated temperature during composting routinely exceeds 50 °C.

Scheme 2. Schematic Illustration of the Arrangement of the Polar Layers for PBS (a) and PBG (b). The Arrows Indicate the Direction of Polarization

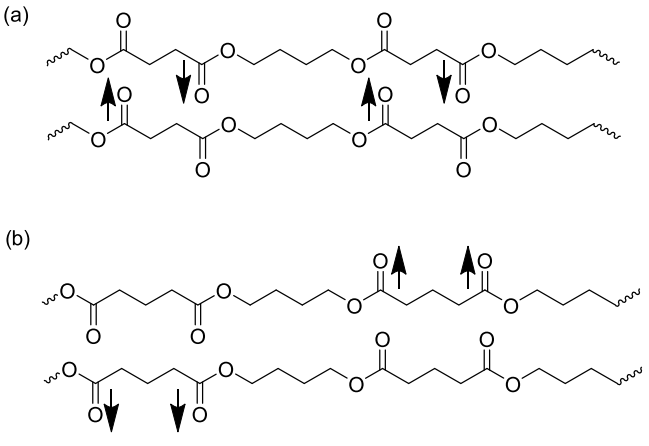

4.2. Thermal Properties of PLA/PBG Blends. Figure 2 shows the second heating DSC thermograms of neat PLA, PBG, and subsequent blends. The first heating and cooling curves are presented in Figures S5 and S6. All DSC curves in Figure 2 displayed three thermal transitions: T_m, T_g, and T_{cc}. The detailed results of DSC are summarized in Table S3, as these thermal transitions can be used to differentiate the miscibility of the blends. A miscible blend is characterized by a single thermal transition, while an immiscible blend is characterized by multiples thermal transitions for each polymer. PLA/PBG blends showed a single T_m below an addition level of 3 wt % of PBG. However, for higher concentrations of PBG, two independent melting transitions for PLA and PBG are observed, which is evidence for phase separation in PBG loading above 3 wt %.

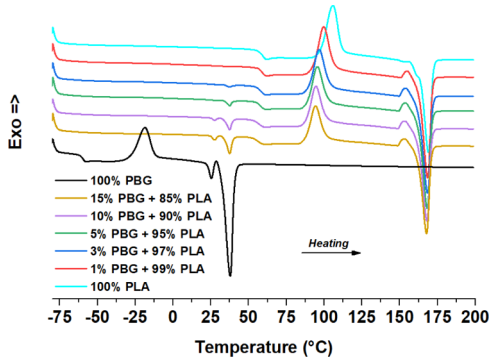

Figure 2. DSC thermograms of the second heating cycle of PLA and PLA/PBG blends.

From the DSC scans shown in Figure 2, PLA has a T_g at 58 °C, T_{cc} at 106 °C, and T_m at 169 °C. The blends containing PBG showed a lower T_g with increasing PBG content. The T_g decreased from 58 °C (neat PLA) to 55 °C (PLA/15 wt % PBG). This indicates that the mobility of PLA chains is slightly enhanced due to the presence of PBG. It is apparent that the addition of PBG also affects T_{cc}. The T_{cc} observed in PLA at 106 °C was decreased to 94 °C with the addition of 15 wt % of PBG, consistent with the lowering of the T_g. The increased chain mobility likely enhances the ability of PLA to cold crystallize at lower temperatures.[18] This result is similar to other plasticized PLA reports with citrate ester plasticizers,[55] ester oligomers,[56] and epoxidized soybean oil.[17] The crystallinity of PLA (X_C%) was calculated from DSC curves using the following equation

$$x_C\% = (\Delta H_m\text{-}\Delta H_{cc}/\Delta H_m^0 X X_{PLA}) \times 100 \quad (1)$$

where ΔH_m was the enthalpy of melting, ΔH_{cc} was the enthalpy of cold crystallization, and X_{PLA} was the weight fraction of PLA in the blends. ΔH_m^0 was the melting enthalpy of 100% crystalline PLA, which is 93 J/g.[57] From Table S3, the degree of crystallinity increased when the PBG content was increased. The crystallinity in neat PLA was 3.1% and increased to 7.5% with the addition of 15 wt % PBG. The degree of crystallinity of PLA/PBG blends was higher than the PLA again likely due to the increased chain mobility.

https://dx.doi.org/10.1021/acsapm.1c00078
ACS Appl. Polym. Mater. 2021, 3, 1652−1663

Table 1. DMA Data of PLA/ PBG Blends

sample	PLA/PBG content (wt %)	storage modulus (MPa)	T_g (°C)	loss modulus (at the beginning) (MPa)	loss modulus (top peak) (MPa)	tan delta (top peak)
1	100/0	2984	52.3	81.3	533.6	2.4
2	99/1	2968	50.2	78.3	473.2	2.5
3	97/3	2913	49.3	75.7	518.9	2.3
4	95/5	2847	48.8	78.1	489.4	2.4
5	90/10	2547	47.6	76.5	431.3	2.4
6	85/15	2311	46.2	78.6	372.7	2.2

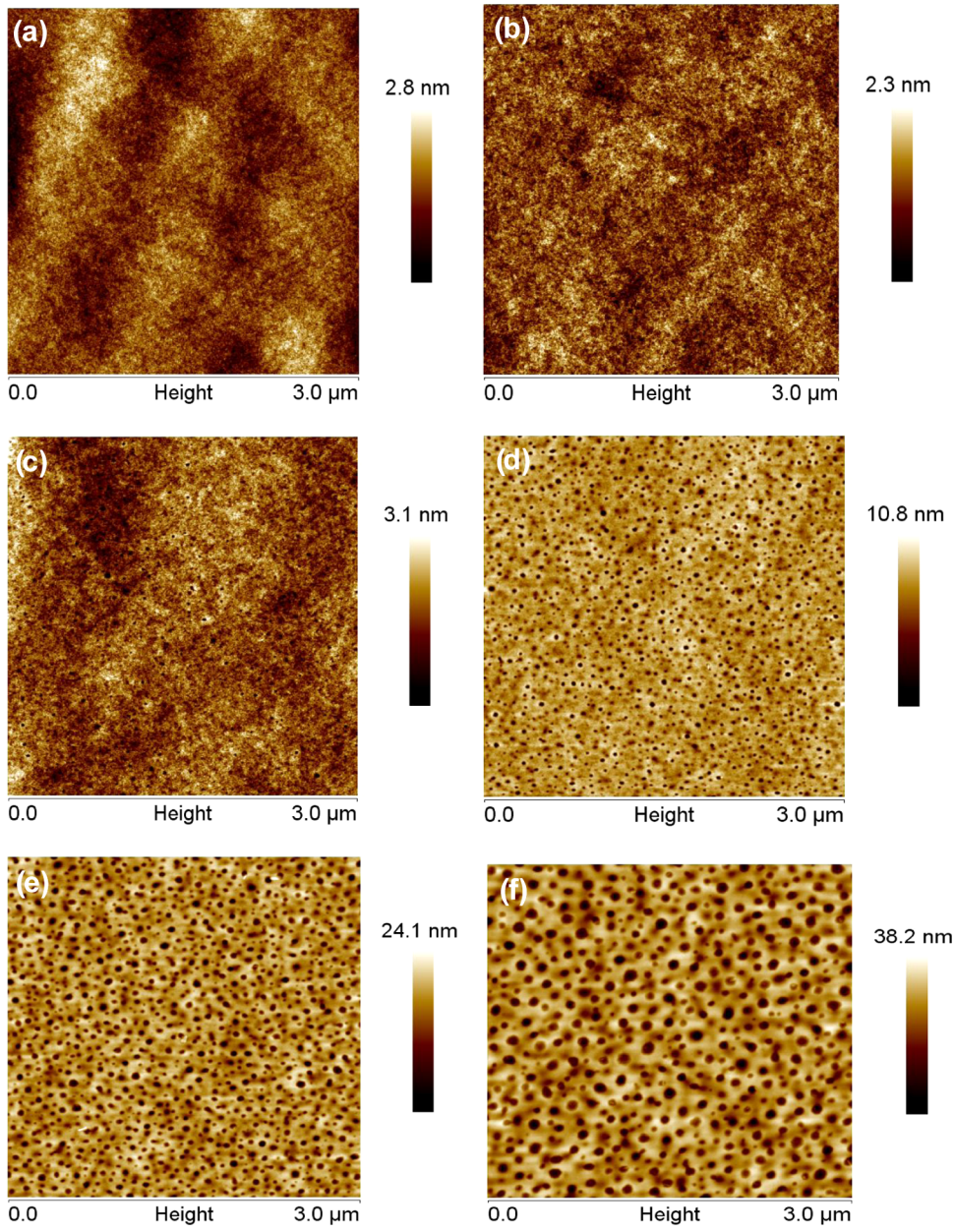

Figure 3. AFM height images of spin-coated films of the PLA and PLA/PBG blends: (a) neat PLA, (b) 1% PBG + 99% PLA, (c) 3% PBG + 97% PLA, (d) 5% PBG + 95% PLA, (e) 10% PBG + 90% PLA, and (f) 15% PBG + 85% PLA.

4.3. Viscoelastic Behavior of PLA/PBG Blends. Figure S7 shows the storage modulus (E'), loss modulus (E''), and tan delta ($\tan\delta$) as a function of temperature, as measured by dynamic mechanical analysis (DMA). In Figure S7, the E' of all samples decreased with increasing temperature below 60 °C. There was a significant drop of E' in the regions between 50 and 60 °C as the material enters the glass transition, indicating an increase in the mobility of the polymer. Between 60 and 90 °C, the E' curves displayed a short plateau that starts to rise around 90 °C due to the onset of cold crystallization.[17,58,59] When comparing PLA and PLA/PBG blends, the E′ of the PLA/PBG blends exhibited lower values,

https://dx.doi.org/10.1021/acsapm.1c00078
ACS Appl. Polym. Mater. 2021, 3, 1652−1663

decreasing with increasing PBG content from 2984 MPa (neat PLA) to 2311 MPa (PLA/15 wt % PBG). In addition, the T_g observed by DMA decreases with increasing PBG content. The T_g of PLA was 52.3 °C, and 15 wt % PBG decreased the T_g to 46.2 °C, consistent with that observed from DSC.

The E'' curves are displayed in Figure S7, which demonstrate that the peak intensity of E'' in the PLA/PBG blends is lower than neat PLA. The peak intensity of E'' is related to the melt viscosity of a polymer,[60] and the shifting of the E'' peak can be associated with a decreased melt viscosity in the blends. It was observed that the E'' for neat PLA is 533.6 MPa and decreased to 372.7 MPa for PLA/15 wt % PBG. The tan δ also shifts to lower temperature with increasing PBG content in the blends. All of the DMA data is summarized in Table 1.

4.4. Miscibility of PLA/PBG Blends. The AFM topography of different blend compositions in which the amount of PBG was varied between 1 and 15 wt % are shown in Figure 3. Microvoids were readily observed when PLA was blended with PBG above 3 wt %. This is also evidence of phase separation and corroborates the observations from DSC, where multiple thermal transitions were observed. Since the solubility of the two components in the solution are different and the interfacial adhesion between PBG and PLA is relatively poor, PBG aggregated and formed microvoids in the PLA matrix during the film-forming process.[61,62] The average height and diameter of the holes increased with an increasing amount of PBG. Table S4 reports the film thickness, height, and diameters of the voids.

To confirm the morphological observations, *AFM-IR was* used to identify and map polymer components in the blends. Figure S8 shows AFM height images and IR mapping images of PLA with 15 wt % PBG taken at 1730 and 1760 cm^{-1}, which can be assigned to the *carbonyl* stretching vibration band of PBG and PLA components, respectively (Figure S9). As seen in these IR mapping images, the IR absorption at 1730 cm^{-1} is dominant in the microvoids, whereas it is weak in the ridge areas. In contrast, the ridge regions show a high IR absorption at 1760 cm^{-1} due to the high density of carbonyl groups of PLA. This result further suggests that PLA and PBG are immiscible.

Like all other polymer classes, PLA blended with other polymers are either partially miscible or immiscible, and their mechanical properties depend strongly on this miscibility.[63,64] PLA/PBS blends also demonstrate an immiscible phase structure, which resulted in an unsatisfactory toughening effect.[27] The main challenge with immiscible polymer blends is improving the adhesion between the blended components or reducing the dispersed phase domain size. For this reason, compatibilizers are typically added to improve the properties of the blend. Compatibilization of polymer blends was not attempted in this study but likely can be used to further improve the miscibility (and subsequent toughness) in these composites.

4.5. Tensile Properties of PLA/PBG Blends. Tensile strength, tensile modulus, and % elongation at break of pure PLA, various PLA/PBG blends, and various PLA/PBS blends are shown in Table S5. A typical stress−strain curve for the blends is also shown in Figure 4. The inclusion of PBG in PLA decreases the tensile strength and tensile modulus but increases the % elongation at break. The tensile modulus of neat PLA exhibited the highest value (3.4 GPa) compared to the blends. The elongation at break of PLA/PBG increased from 2.5 to 21.6% with 15 wt % of PBG. The increase in

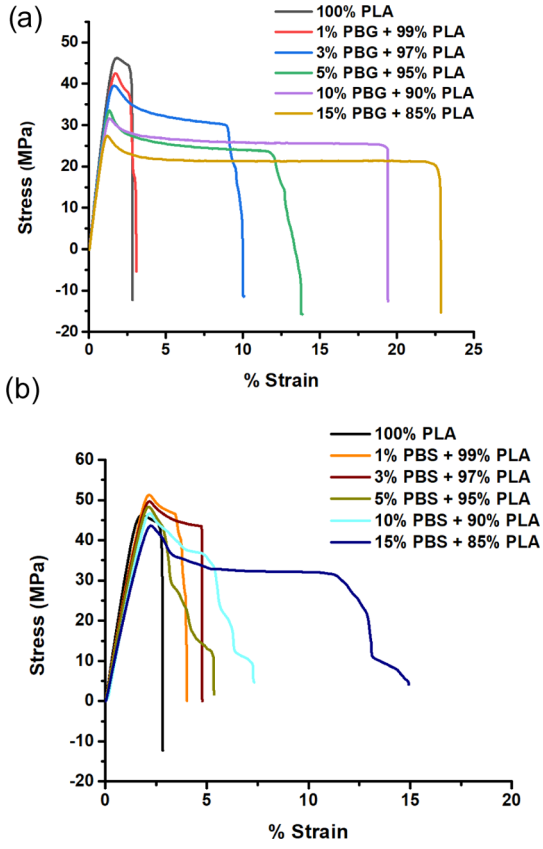

Figure 4. Stress−strain curves for (a) PLA/PBG blends and (b) PLA/PBS blends.

ductility suggests that the PLA/PBG blends become more flexible with increasing PBG content.

The same trends in tensile strength, tensile modulus, and % elongation at break were also observed in the PLA/PBS blends. According to our observations, a higher concentration of PBS in the PLA matrix is necessary to achieve the same improvement in toughness. The addition of 5 and 15% of PBS into the PLA matrix improved the % elongation at break by 5.0 and 13.2%, respectively. These results suggested that the brittleness of PLA can be adjusted by blending with PBS. Interestingly, PLA/PBG blends exhibit higher ductility than PLA/PBS blends under the same loadings. The PLA/PBG blend had a 14.9% elongation at break with only 5% of PBG, while the PLA/PBS blend had a similar elongation at break (13.2%) at a loading of 15% PBS.

Regarding the stress−strain curve, the deformation and fracture behavior of the neat PLA can be considered as the resistance to stretching of polymer chain networks. By adding PBG, the mobility of PLA chains is enhanced and the resistance to stretching decreases, resulting in a reduced tensile modulus and tensile strength. Moreover, there is recognizable yielding behavior and strain softening of all PLA/PBG blends. Stain softening is a gradual decline of stress at increasing strain, which is primarily a consequence of the brittleness and heterogeneity of the material.[65]

During the tensile testing, PLA/PBG blends exhibited a stress-whitening effect,[66] whereas PLA/PBS did not (Figures S10 and S11). This crazing occurred when the samples were deformed, decreasing their transparency and becoming opaque in appearance. The microvoids[67] that were observed with AFM are likely responsible for the initiation of this "whitening"

https://dx.doi.org/10.1021/acsapm.1c00078
ACS Appl. Polym. Mater. 2021, 3, 1652−1663

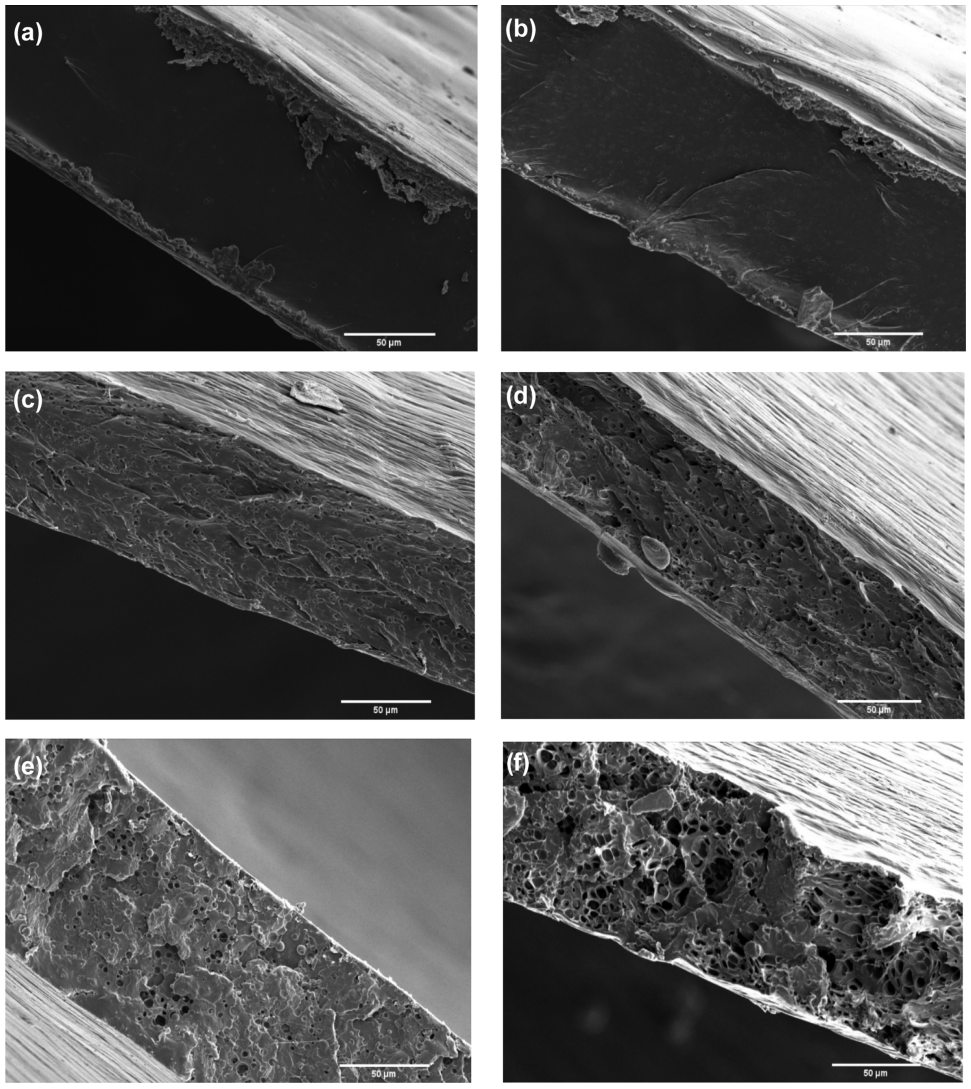

Figure 5. SEM cross-sectional images of tensile bar fracture surface of PLA and PLA/PBG blends: (a) neat PLA, (b) 1% PBG + 99% PLA, (c) 3% PBG + 97% PLA, (d) 5% PBG + 95% PLA, (e) 10% PBG + 90% PLA, and (f) 15% PBG + 85% PLA.

effect. Under enough mechanical loading, the tensile stress applied is concentrated at the interface of the microvoids, and as a result, the microvoids increase in size and allow for the alignment of microfibrils between voids. The aligned structure enables the fibrils to carry the applied stress until breaking. The extensive stress is dissipated by crazing and postpones the ultimate failure of the material.[11] To explore the toughness mechanism, SEM was used to study the fracture surface of the specimens.

4.6. Morphology of PLA/PBG Blends. Figure 5 (and also S12) shows the SEM images of the tensile test fracture surface of the PLA/PBG blends. The fracture surface of neat PLA is very smooth and uniform, as expected with no phase separation. The fracture surface of the blends appears rougher and the formation of microvoids with increasing PBG content are obvious. The void size continues to grow with stress loading during the tensile test. This visible increase in void formation correlates well with the AFM analysis. As the PBG content increases, the appearance of more voids is observed due to an increase in phase separation. The increase in void size with increasing PBG content also correlates well with the tensile testing data. Samples that have higher PBG loading demonstrate longer elongation at break due to void growth and alignment of microfibrils. The average void size for blends with 1, 3, 5, 10, and 15% PBG were 0.5−1, 1−2, 2−3, 3.5−4.5, and 7−8 μm, respectively. This increase in void size coupled with an increased elongation at break confirms that as the void grows, it allows for the alignment of microfibrils, which results in greater stress dissipation and better toughness.

4.7. Aerobic Composting Biodegradability of PLA/PBG Blends. The composting biodegradability of PLA and PLA-based blends were investigated by respirometry to determine the influence of PBG on PLA degradation. In general, it is our observation that the blending of polymers influences the overall degradation behavior of the blend and typically differs from the degradation rate of the neat components alone. The interaction among different species in the blends and overall morphology influence the diffusion rate of water and subsequent hydrolytic reactions during degradation.[68] Because of space limitations in the respirometer and the best performance of toughness, the blend of 15% PBG and 85% PLA was selected for respirometry evaluation. The carbon and nitrogen contents of PLA were 52.5 and 0.03% and the blend were 53.3 and 0.01%, respectively. The compost

https://dx.doi.org/10.1021/acsapm.1c00078
ACS Appl. Polym. Mater. 2021, 3, 1652−1663

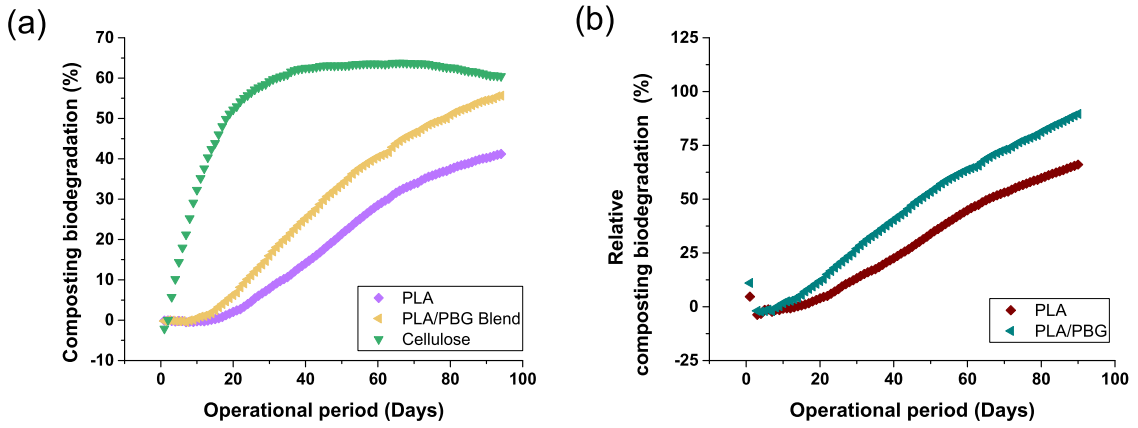

Figure 6. Degradability of cellulose (reference material), PLA, and PLA blended with 15% PBG. (a) Composting biodegradation; (b) relative composting biodegradation.

inoculum that used in this experiment had pH of 8.0, total solid of 51.7 wt % of the wet solid, and volatile solid of 17.7 wt % of the wet solid. The total carbon to nitrogen ratio (C/N) of the compost inoculum was 19.2.

All of the emitted CO_2 was monitored and quantified during the composting degradation test. The percent of composting biodegradation can be calculated by dividing the actual CO_2 emission from the samples by the theoretical CO_2 emission from the samples and multiplying by 100. After 90 days under a controlled composting aerobic condition in a respirometer operated at 58 °C, the composting biodegradation of PLA was 40.2% PLA and the blend reached 54.5% (Figure 6a). The relative composting biodegradation of PLA and the blend was 66.1 and 89.6%, respectively (Figure 6b). The results showed that the composting biodegradation of this blend degraded faster than the neat PLA and it passed the threshold limit requirement for biodegradation imposed by the ASTM standard D6400-12,[69] which states that the biodegradability must reach at least 90% relative to cellulose within 180 days.

4.8. Modified Gompertz Model. Using the modified Gompertz model to fit sample CO_2 production, the composting biodegradation of each test specimen can compare quantitatively through two different composting experiments. This compost inoculum was sourced from the same industrial composting facility and from comparable 4−5 months old compost. The PBG and PBS were studied against the "Cellulose 1" positive control, while the PLA and PLA/PBG blend were examined against the "Cellulose 2" positive control in a later experiment. The difference in CO_2 production between the blank controls and any test material reveals the amount of gaseous carbon loss from each sample, as shown in Figure 7.

Notably, the cumulative yield of the cellulose controls in the PBG and PBS respirometry experiments displayed higher cumulative CO_2 yield than the cellulose controls in the PLA and PLA/PBG blend respirometry experiment. This observation also helps describe the activity of the compost inoculum, whereby the inoculum in the PBG and PBS testing likely had higher overall activity on the cellulose control and the test samples when compared to the separate PLA and PLA/PBG blend respirometry experiments. The maximum CO_2 potential (P_m) was 737.1 and 566.5 mL $CO_2 \cdot g^{-1}$ sample for Cellulose 1 and Cellulose 2 positive controls, respectively, verifying the higher inoculum activity of the first composting experiment.

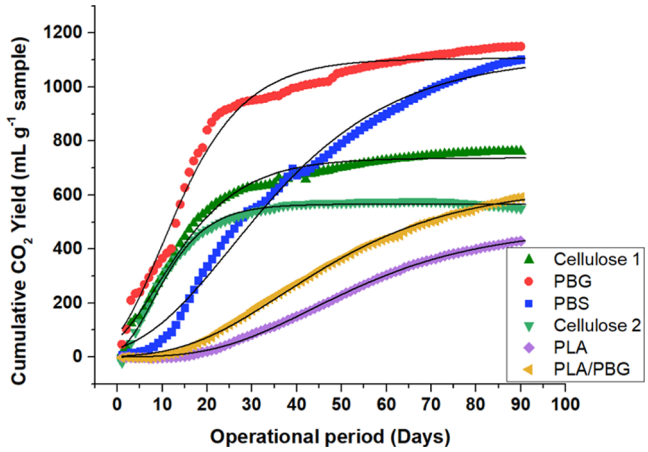

Figure 7. Gaseous carbon loss from samples. The cumulative CO_2 production is plotted for each operational day for the two respirometry experiments. Note that Cellulose 1 is the positive control for the PBG and PBS composting experiment and Cellulose 2 is the positive control for the PLA and PLA/PBG blend composting experiment. Dotted lines represent the modified Gompertz models according to the corresponding parameters in Table 2.

Modified Gompertz kinetic parameters and absolute biodegradation of PBG, PBS, PLA, and 15% PBG + 85% PLA are shown in Table 2. PBG returned the fastest rate of biodegradation (39.7 mL $CO_2 \cdot d^{-1}$), even faster than the cellulose controls in the respirometry experiments. By extension, the PBG/PLA blend also yielded a faster rate of biodegradation (10.7 mL $CO_2 \cdot d^{-1}$) than the PLA alone (8.2 mL $CO_2 \cdot d^{-1}$). The increase in the rate of biodegradation and the decrease in the hydrolysis lag-phase time observed in the PLA/PBG blend when compared to the PLA suggests that the PLA/PBG blend will have better industrial composting outcomes than PLA.

During the initial degradation period, there was a very short lag-phase period. The lag-phase time for cellulose and PBG returned negative values of −1.3 and −0.5 days, respectively. This occurs in situations where bioproducts (CO_2 was monitored in this experiment) are generated almost instantaneously without a lag period.[70] This is not surprising for the cellulose control considering the compost inoculum is primarily composed of lignocellulosic biomass where endogenous cellulase enzymes are abundant; however, the PBG also returned a negative lag-phase time, suggesting this polymer is

https://dx.doi.org/10.1021/acsapm.1c00078
ACS Appl. Polym. Mater. 2021, 3, 1652−1663

Table 2. Modified Gompertz Model Parameters of CO_2 Production and Gaseous Carbon Loss from Samples

parameters	cellulose 1	PBG	PBS	cellulose 2	PLA	85% PLA+ 15% PBG
P_m (mL $CO_2 \cdot g^{-1}$ sample)	737.1	1106.0	1115.0	566.5	481.6	635.4
R_m (mL $CO_2 \cdot d^{-1}$)	26.2	39.7	20.3	31.1	8.2	10.7
λ (day)	−1.3	−0.5	5.4	1.2	21.7	15.0
CO_2 yield (mL $CO_2 \cdot g^{-1}$ sample)	762.8	1151.4	1104.8	547.0	439.8	603.4
absolute biodegradation (%)	87.4[a]	94.1[a]	90.8[a]	60.5[b]	41.2[b]	55.7[b]
biodegradation relative to cellulose (%)	N/A	107.6[a]	103.9[a]	N/A[b]	66.1[b]	89.6[b]

[a]Biodegradation values determined after 90 days of testing against Cellulose 1. [b]Biodegradation values determined after 90 days of testing against Cellulose 2.

readily deconstructed instantaneously in thermophilic composting inoculum. The instantaneous biodegradation of PBG is likely associated with both abiotic and enzymatic hydrolysis processes to afford the fast metabolism of the carbon into CO_2.

5. CONCLUSIONS

In this work, PBG was successfully synthesized through a melt polycondensation reaction and can be sourced using 100% bio-based monomers. PBG is readily compostable and blending PBG with PLA improves the PLA brittleness without compromising its degradability. The thermal properties of PBG demonstrate a lower T_g and T_m when compared to PBS due to the odd carbon atom in the diacid repeat unit, which ultimately increases the degradation rate of PBG. The blends of PLA and PBG were prepared with various compositions via solution casting and were fully characterized by thermal and mechanical testing along with AFM and SEM. The blends of PBG exhibit phase separation above 3% and enhance the mobility of PLA chains in the matrix. The tensile toughness of the blends is increased without compromising the tensile strength or modulus of PLA. The composting biodegradation also showed that the PBG/PLA blend had a faster degradation rate than the neat PLA during the testing period. Further work on copolymer compatibilizers is ongoing, which aims at enhancing the adhesion strength between the two components and manipulating the phase domain size, which will allow further tuning of the ultimate mechanical properties and rates of composting biodegradation.

■ ASSOCIATED CONTENT

Supporting Information

The Supporting Information is available free of charge at https://pubs.acs.org/doi/10.1021/acsapm.1c00078.

Additional experimental details and figures, including acid number, ^{1}H NMR, TGA, DSC, DMA, FTIR, AFM-IR, SEM, tensile properties, compost properties, surface morphologies of cast films, sample preparation for SEM, measurement of biogas production, and calculation of modified Gompertz kinetics (PDF)

■ AUTHOR INFORMATION

Corresponding Author

Jason Locklin − *Department of Chemistry, New Materials Institute, and College of Engineering, University of Georgia, Athens, Georgia 30602, United States;* orcid.org/0000-0001-9272-2403; Email: jlocklin@uga.edu

Authors

Apisata Holt − *Department of Chemistry and New Materials Institute, University of Georgia, Athens, Georgia 30602, United States*

Yutian Ke − *Department of Chemistry and New Materials Institute, University of Georgia, Athens, Georgia 30602, United States*

Jessica A. Bramhall − *New Materials Institute and College of Engineering, University of Georgia, Athens, Georgia 30602, United States*

Grant Crane − *Department of Chemistry and New Materials Institute, University of Georgia, Athens, Georgia 30602, United States*

Joe B. Grubbs, III − *New Materials Institute, University of Georgia, Athens, Georgia 30602, United States*

Evan M. White − *New Materials Institute, University of Georgia, Athens, Georgia 30602, United States;* orcid.org/0000-0002-9083-1072

Jessica Horn − *New Materials Institute, University of Georgia, Athens, Georgia 30602, United States*

Complete contact information is available at: https://pubs.acs.org/10.1021/acsapm.1c00078

Notes

The authors declare no competing financial interest.

■ ACKNOWLEDGMENTS

This work was supported by the Center for Bioplastics and Biocomposites under the National Science Foundation grant no. 1841319.

■ REFERENCES

(1) Ishida, N.; Saitoh, S.; Ohnishi, T.; Tokuhiro, K.; Nagamori, E.; Kitamoto, K.; Takahashi, H. Metabolic engineering of Saccharomyces cerevisiae for efficient production of pure L-(+)-lactic acid. *Appl. Biochem. Biotechnol.* **2006**, *131*, 795−807.

(2) Cheng, Y.; Deng, S.; Chen, P.; Ruan, R. Polylactic acid (PLA) synthesis and modifications: A review. *Front. Chem. China* **2009**, *4*, 259−264.

(3) Auras, R.; Harte, B.; Selke, S. An overview of polylactides as packaging materials. *Macromol. Biosci.* **2004**, *4*, 835−64.

(4) Garlotta, D. A Literature Review of Poly(Lactic Acid). *J. Polym. Environ.* **2001**, *9*, 63−84.

(5) Lim, L.-T.; Auras, R.; Rubino, M. Processing technologies for poly (lactic acid). *Prog. Polym. Sci.* **2008**, *33*, 820−852.

(6) Williams, C. K.; Hillmyer, M. A. Polymers from Renewable Resources: A Perspective for a Special Issue of Polymer Reviews. *Polym. Rev.* **2008**, *48*, 1−10.

(7) Li, H.; Huneault, M. A. Effect of nucleation and plasticization on the crystallization of poly (lactic acid). *Polymer* **2007**, *48*, 6855−6866.

(8) Huneault, M. A.; Li, H. Morphology and properties of compatibilized polylactide/thermoplastic starch blends. *Polymer* **2007**, *48*, 270−280.

(9) Grijpma, D. W.; Nijenhuis, A. J.; Van Wijk, P. G. T.; Pennings, A. J. High impact strength as-polymerized PLLA. *Polym. Bull.* **1992**, *29*, 571−578.

(10) Liu, H.; Zhang, J. Research progress in toughening modification of poly (lactic acid). *J. Polym. Sci., Part B: Polym. Phys.* **2011**, *49*, 1051−1083.
(11) Kfoury, G.; Raquez, J.; Hassouna, F.; Odent, J.; Toniazzo, V.; Ruch, D.; Dubois, P. Recent advances in high performance poly (lactide): from "green" plasticization to super-tough materials via (reactive) compounding. *Front. Chem.* **2013**, *1*, 1−46.
(12) Tokiwa, Y.; Calabia, B. P.; Ugwu, C. U.; Aiba, S. Biodegradability of Plastics. *Int. J. Mol. Sci.* **2009**, *10*, 3722−3742.
(13) Xie, L.; Xu, H.; Niu, B.; Ji, X.; Chen, J.; Li, Z. M.; Hsiao, B. S.; Zhong, G. J. Unprecedented Access to Strong and Ductile Poly(lactic acid) by Introducing In Situ Nanofibrillar Poly(butylene succinate) for Green Packaging. *Biomacromolecules* **2014**, *15*, 4054−4064.
(14) Hosseinnezhad, R.; Vozniak, I.; Morawiec, J.; Galeski, A.; Dutkiewicz, S. In situ generation of sustainable PLA-based nanocomposites by shear induced crystallization of nanofibrillar inclusions. *RSC Adv.* **2019**, *9*, 30370−30380.
(15) Labrecque, L.; Kumar, R.; Dave, V.; Gross, R.; McCarthy, S. Citrate Esters as Plasticizers for poly (lactic acid). *J. Appl. Polym. Sci.* **1997**, *66*, 1507−1513.
(16) Ljungberg, N.; Wesslén, B. The Effects of Plasticizers on the Dynamic Mechanical and Thermal Properties of poly(lactic acid). *J. Appl. Polym. Sci.* **2002**, *86*, 1227−1234.
(17) Ali, F.; Chang, Y.; Kang, S.; Yoon, J. Thermal, mechanical and rheological properties of poly (lactic acid)/epoxidized soybean oil blends. *Polym. Bull.* **2009**, *62*, 91−98.
(18) Kulinski, Z.; Piorkowska, E. Crystallization, structure and properties of plasticized poly (L-lactide). *Polymer* **2005**, *46*, 10290−10300.
(19) Sheth, M.; Kumar, R. A.; Davé, V.; Gross, R. A.; McCarthy, S. P. Biodegradable Polymer Blends of Poly (lactic acid) and Poly (ethylene glycol). *J. Appl. Polym. Sci.* **1997**, *66*, 1495−1505.
(20) Zhang, L.; Xiong, C.; Deng, X. Biodegradable Polyester Blends for Biomedical Application. *J. Appl. Polym. Sci.* **1995**, *56*, 103−112.
(21) Park, J. W.; Im, S. S. Phase Behavior and Morphology in Blends of poly (L-lactic acid) and Poly (butylene succinate). *J. Appl. Polym. Sci.* **2002**, *86*, 647−655.
(22) Jiang, L.; Wolcott, M. P.; Zhang, J. Study of Biodegradable Polylactide/Poly(butylene adipate-co-terephthalate) blends. *Biomacromolecules* **2006**, *7*, 199−207.
(23) Vieira, M. G. A.; da Silva, M. A.; dos Santos, L. O.; Beppu, M. M. Natural-based plasticizers and biopolymer films: A review. *Eur. Polym. J.* **2011**, *47*, 254−263.
(24) An, Y.; Ding, Y.; Tan, J.; Yang, W. Influences of Polyester Plasticizers on the Properties of Oil Resistance Flexible Poly (vinyl chloride) and Powder Nitrile Butadiene Rubber Blends. *Adv. Sci. Lett.* **2011**, *4*, 875−879.
(25) Jia, P.; Xia, H.; Tang, K.; Zhou, Y. Plasticizers Derived from Biomass Resources: A Short Review. *Polymers* **2018**, *10*, 1303.
(26) Wang, R.; Wang, S.; Zhang, Y.; Wan, C.; Ma, P. Toughening Modification of PLLA/PBS Blends via in Situ Compatibilization. *Polym. Eng. Sci.* **2009**, *49*, 26−33.
(27) Su, S.; Kopitzky, R.; Tolga, S.; Kabasci, S. Polylactide (PLA) and Its Blends with Poly(butylene succinate) (PBS): A Brief Review. *Polymers* **2019**, *11*, 1193.
(28) Bhatia, A.; Gupta, R. K.; Bhattacharya, S. N.; Choi, H. J. Compatibility of biodegradable poly (lactic acid)(PLA) and poly (butylene succinate)(PBS) blends for packaging application. *Korea-Australia Rheol. J.* **2007**, *19*, 125−131.
(29) Hassan, E.; Wei, Y.; Jiao, H.; Muhuo, Y. Informatics, Dynamic Mechanical Properties and Thermal Stability of Poly (lactic acid) and Poly (butylene succinate) blends Composites. *J. Fiber Bioeng. Inform.* **2013**, *6*, 85−94.
(30) Wcisłek, A.; Sonseca Olalla, A.; McClain, A.; Piegat, A.; Sobolewski, P.; Puskas, J.; El Fray, M. Enzymatic Degradation of Poly (butylene succinate) Copolyesters Synthesized with the Use of Candida antarctica Lipase B. *Polymers* **2018**, *10*, 688.
(31) Muthuraj, R.; Misra, M.; Mohanty, A. K. Hydrolytic degradation of biodegradable polyesters under simulated environmental conditions. *J. Appl. Polym. Sci.* **2015**, *132*, 42189.
(32) Benali, S.; Aouadi, S.; Dechief, A.; Murariu, M.; Dubois, P. Key factors for tuning hydrolytic degradation of polylactide/zinc oxide nanocomposites. *Nanocomposites* **2015**, *1*, 51−61.
(33) Haider, T. P.; Völker, C.; Kramm, J.; Landfester, K.; Wurm, F. R. Plastics of the Future? The Impact of Biodegradable Polymers on the Environment and on Society. *Angew. Chem., Int. Ed.* **2019**, *58*, 50−62.
(34) Siparsky, G. L.; Voorhees, K. J.; Dorgan, J. R.; Schilling, K. Water Transport in Polylactic Acid (PLA), PLA/Polycaprolactone Copolymers, and PLA/Polyethylene Glycol Blends. *J. Environ. Polym. Degrad.* **1997**, *5*, 125−136.
(35) Wang, Y.; Xiao, Y.; Duan, J.; Yang, J.; Wang, Y.; Zhang, C. Accelerated hydrolytic degradation of poly(lactic acid) achieved by adding poly(butylene succinate). *Polym. Bull.* **2016**, *73*, 1067−1083.
(36) Bunn, C. W. The Melting Points of Chain Polymers. *J. Polym. Sci.* **1955**, *16*, 323−343.
(37) Woodard, L. N.; Grunlan, M. A. Hydrolytic Degradation and Erosion of Polyester Biomaterials. *ACS Macro Lett* **2018**, *7*, 976−982.
(38) Jansen, M. L.; van Gulik, W. M. Towards large scale fermentative production of succinic acid. *Curr. Opin. Biotechnol.* **2014**, *30*, 190−197.
(39) Stadler, B. M.; Wulf, C.; Werner, T.; Tin, S.; de Vries, J. G. Catalytic Approaches to Monomers for Polymers Based on Renewables. *ACS Catal.* **2019**, *9*, 8012−8067.
(40) Li, W.; Ma, L.; Shen, X.; Wang, J.; Feng, Q.; Liu, L.; Zheng, G.; Yan, Y.; Sun, X.; Yuan, Q. Targeting metabolic driving and intermediate influx in lysine catabolism for high-level glutarate production. *Nat. Commun.* **2019**, *10*, No. 3337.
(41) Wang, J.; Wu, Y.; Sun, X.; Yuan, Q.; Yan, Y. De Novo Biosynthesis of Glutarate via α-Keto Acid Carbon Chain Extension and Decarboxylation Pathway in Escherichia coli. *ACS Synth. Biol.* **2017**, *6*, 1922−1930.
(42) Isikgor, F. H.; Becer, C. R. Lignocellulosic biomass: a sustainable platform for the production of bio-based chemicals and polymers. *Polym. Chem.* **2015**, *6*, 4497−4559.
(43) ASTM Standard D5338-15. Standard test method for determining aerobic biodegradation of plastic materials under controlled composting conditions, incorporating thermophilic temperatures. ASTM International: West Conshohocken, PA, 2015.
(44) Kirsten, W. J. Automatic Methods for the Simultaneous Determination of Carbon, Hydrogen, Nitrogen, and Sulfur, and for Sulfur Alone in Organic and Inorganic materials. *Anal. Chem.* **1979**, *51*, 1173−1179.
(45) Wang, S.; Lydon, K. A.; White, E. M.; Grubbs, J. B.; Lipp, E. K.; Locklin, J.; Jambeck, J. R. Biodegradation of Poly(3-hydroxybutyrate-co-3-hydroxyhexanoate) Plastic under Anaerobic Sludge and Aerobic Seawater Conditions: Gas Evolution and Microbial Diversity. *Environ. Sci. Technol.* **2018**, *52*, 5700−5709.
(46) Yoon, Y.; Kim, S.; Oh, S.; Kim, C. Potential of anaerobic digestion for material recovery and energy production in waste biomass from a poultry slaughterhouse. *Waste Manage.* **2014**, *34*, 204−209.
(47) Costa, J. C.; Barbosa, S. G.; Alves, M. M.; Sousa, D. Z. Thermochemical pre-and biological co-treatments to improve hydrolysis and methane production from poultry litter. *Bioresour. Technol.* **2012**, *111*, 141−147.
(48) Zwietering, M. H.; Jongenburger, I.; Rombouts, F. M.; van 't Riet, K. Modeling of the Bacterial Growth Curve. *Appl. Environ. Microbiol.* **1990**, *56*, 1875−1881.
(49) Nisoli, A.; Doherty, M. F.; Malone, M. F. Feasible Regions for Step-Growth Melt Polycondensation Systems. *Ind. Eng. Chem. Res.* **2004**, *43*, 428−440.
(50) Gupta, S. K.; Kumar, A. *Reaction Engineering of Step Growth Polymerization*; Plenum Press: New York, 1987.

https://dx.doi.org/10.1021/acsapm.1c00078
ACS Appl. Polym. Mater. 2021, 3, 1652−1663

(51) Bhaumik, D.; Mark, J. E. Odd-even variations in the melting points of some ethylene polyesters. *Makromol. Chem.* **1986**, *187*, 1329−1334.
(52) Rickert, S. E.; Baer, E.; Wittmann, J. C.; Kovacs, A. J. Epitaxial Crystallization of Polyesters on Inorganic and Organic Substrates. *J. Polym. Sci., Polym. Phys. Ed.* **1978**, *16*, 895−906.
(53) Stempfle, F.; Ortmann, P.; Mecking, S. Long-Chain Aliphatic Polymers To Bridge the Gap between Semicrystalline Polyolefins and Traditional Polycondensates. *Chem. Rev.* **2016**, *116*, 4597−4641.
(54) Korshak, V. V.; Vinogradova, S. V. *Polyesters*; Pergamon Press: New York, 1965.
(55) Maiza, M.; Benaniba, M. T.; Quintard, G.; Massardier-Nageotte, V. Biobased additive plasticizing Polylactic acid (PLA). *Polimeros* **2015**, *25*, 581−590.
(56) Cicogna, F.; Coiai, S.; De Monte, C.; Spiniello, R.; Fiori, S.; Franceschi, M.; Braca, F.; Cinelli, P.; Fehri, S. M. K.; Lazzeri, A.; Oberhauser, W.; Passaglia, E. Poly(lactic acid) plasticized with low-molecular-weight polyesters: structural, thermal and biodegradability features. *Polym. Int.* **2017**, *66*, 761−769.
(57) Fischer, E. W.; Sterzel, H. J.; Wegner, G. Investigation of the structure of solution grown crystals of lactide copolymers by means of chemical reactions. *Kolloid-Z. u. Z. Polymere.* **1973**, *251*, 980−990.
(58) Kamthai, S.; Magaraphan, R. In *Thermal and mechanical properties of polylactic acid (PLA) and bagasse carboxymethyl cellulose (CMCB) composite by adding isosorbide diesters* AIP Conference Proceedings, Jana, S. C.; Jana, S. C., Eds., 2015; p 060006.
(59) Shi, X.; Zhang, G.; Phuong, T. V.; Lazzeri, A. Synergistic Effects of Nucleating Agents and Plasticizers on the Crystallization Behavior of Poly(lactic acid). *Molecules* **2015**, *20*, 1579−1593.
(60) Silverajah, V. S. G.; Ibrahim, N. A.; Yunus, W. M. Z. W.; Hassan, H. A.; Buong, W. C. A Comparative Study on the Mechanical, Thermal and Morphological Characterization of Poly(lactic acid)/Epoxidized Palm Oil Blend. *Int. J. Mol. Sci.* **2012**, *13*, 5878−98.
(61) Dalnoki-Veress, K.; Forrest, J. A.; Stevens, J. R.; Dutcher, J. R. Phase separation morphology of spin-coated polymer blend thin films. *Phys. A* **1997**, *239*, 87−94.
(62) Heriot, S. Y.; Jones, R. A. L. An interfacial instability in a transient wetting layer leads to lateral phase separation in thin spin-cast polymer-blend films. *Nat. Mater.* **2005**, *4*, 782−786.
(63) Krause, S. Polymer Compatibility. *J. Macromol. Sci., Polym. Rev.* **1972**, *7*, 251−314.
(64) Sangeetha, V. H.; Deka, H.; Varghese, T. O.; Nayak, S. K. State of the Art and Future Prospectives of poly (Lactic acid) Based Blends and Composites. *Polym. Compos.* **2018**, *39*, 81−101.
(65) Vignjevic, R.; Djordjevic, N.; Vuyst, T. D.; Gemkow, S. Modelling of strain softening materials based on equivalent damage force. *Comput. Methods Appl. Mech. Eng.* **2018**, *335*, 52−68.
(66) Wang, P.; Hutchings, I. M.; Duncan, S. J.; Jenkins, L.; Woo, E. Strain whitening of a thermoplastic olefin material. *J. Mater. Sci.* **2006**, *41*, 4847−4859.
(67) Bagheri, R.; Pearson, R. A. The use of microvoids to toughen polymers. *Polymer* **1995**, *36*, 4883−4885.
(68) La Mantia, F. P.; Morreale, M.; Botta, L.; Mistretta, M. C.; Ceraulo, M.; Scaffaro, R. Degradation of polymer blends: A brief review. *Polym. Degrad. Stab.* **2017**, *145*, 79−92.
(69) ASTM Standard D6400-12. Standard specification for labeling of plastics designed to be aerobically composted in municipal or industrial facilities. ASTM International: West Conshohocken, PA, 2012.
(70) Shen, J.; Zhu, J. Development of General Gompertz Models and Their Simplified Two-Parameter Forms Based on Specific Microbial Growth Rate for Microbial Growth, Bio-Products and Substrate Consumption. *Adv. Biotechnol. Microbiol.* **2017**, *4*, 0064−0074.

https://dx.doi.org/10.1021/acsapm.1c00078
ACS Appl. Polym. Mater. 2021, 3, 1652−1663